
Research Article

Theme: Recent Advances in Musculoskeletal Tissue Engineering
Guest Editor: Aliasger K. Salem

Controlled Ion Release from Novel Polyester/Ceramic Composites Enhances Osteoinductivity

Soheila Ali Akbari Ghavimi,¹ Rama Rao Tata,^{1,4} Andrew J. Greenwald,¹ Brittany N. Allen,² David A. Grant,² Sheila A. Grant,² Mark W. Lee,³ and Bret D. Ulery^{1,2,4}

Received 17 November 2016; accepted 28 February 2017; published online 11 May 2017

Abstract. Due to the growing number of patients suffering from musculoskeletal defects and the limited supply of and sub-optimal outcomes associated with biological graft materials, novel biomaterials must be created that can function as graft substitutes. For bone regeneration, composite materials that mimic the organic and inorganic phases of natural bone can provide cues which expedite and enhance endogenous repair. Specifically, recent research has shown that calcium and phosphate ions are inherently osteoinductive, so controllably delivering their release holds significant promise for this field. In this study, unique aliphatic polyesters were synthesized and complexed with a rapidly decomposing ceramic (monobasic calcium phosphate, MCP) yielding novel polymer/ceramic composite biomaterials. It was discovered that the fast dissolution and rapid burst release of ions from MCP could be modulated depending on polymer length and chemistry. Also, controlled ion release was found to moderate solution pH associated with polyester degradation. When composite biomaterials were incubated with mesenchymal stem cells (MSCs) they were found to better facilitate osteogenic differentiation than the individual components as evidenced by increased alkaline phosphatase expression and more rapid mineralization. These results indicate that controlling calcium and phosphate ion release via a polyester matrix is a promising approach for bone regenerative engineering.

KEY WORDS: calcium/phosphate ions; mesenchymal stem cells; monobasic calcium phosphate; osteoinduction; polyesters.

INTRODUCTION

Musculoskeletal pathologies such as fracture nonunions, osteonecrosis, osteoarthritis, and osteochondral defects are the second leading cause of disability affecting more than 1.7 billion people worldwide (1–3). A fracture nonunion is

defined by the US Food and Drug Administration (FDA) and others as incomplete healing at 9 months after injury and the absence of healing progression over the following three consecutive months (4). Bone grafts (i.e., autografts and allografts) have been utilized for decades as a treatment for nonunion fractures, but problems such as donor scarcity, supply limitation, donor site morbidity, pathogen transfer, and immune-mediated rejection limits their application for large bone defects (5, 6). Tissue engineering offers a promising approach for bone repair with the majority of engineered strategies having shown significant potential in the laboratory, but few solutions have been translated to the clinic (7, 8). A major challenge facing this field is the development of a bone graft substitute which is capable of promoting the differentiation of endogenous stem cells down the osteoblastic lineage (9).

Natural bone is a hierarchically ordered structure with an organic phase matrix (mostly collagen type I) and an inorganic reinforcing phase (mostly hydroxyapatite) (10). A promising bone substitute can mimic natural bone structure by combining an organic matrix with an inorganic, bioactive

Soheila Ali Akbari Ghavimi and Rama Rao Tata contributed equally to this work.

Electronic supplementary material The online version of this article (doi:10.1208/s12248-017-0072-x) contains supplementary material, which is available to authorized users.

¹ Department of Chemical Engineering, University of Missouri, W2027 Laffer Hall, 416 S. 6th Street, Columbia, Missouri 65211, USA.

² Department of Bioengineering, University of Missouri, Columbia, Missouri 65211, USA.

³ Department of Chemistry, University of Missouri, Columbia, Missouri 65211, USA.

⁴ To whom correspondence should be addressed. (e-mail: TataR@missouri.edu; uleryb@missouri.edu)

phase. Composite-based substitutes possess significant clinical potential since they can overcome the limitation associated with each of the individual phases.

The organic phase can consist of naturally derived or synthetic polymers (11, 12). Synthetic polymers with tunable nano-, micro-, and macro-scale properties can be readily synthesized. The main drawbacks of these polymers in bone tissue engineering applications are their limited bioactivity and considerable acidic degradation products, which can hinder the bone regeneration process (13, 14). Polyesters have been well documented for their biodegradable nature, biocompatibility, lack of toxicity, and biocompatible degradation products (15–19). However, poor hydrophilicity and lack of bioactivity require they be modified to function as an ideal bone graft substitute (20). Aliphatic polyesters have been synthesized by several methods, such as direct polycondensation of dicarboxylic acids and diols, ring opening polymerization of cyclic esters, and copolymerization of cyclic anhydrides with epoxides (21–23). Commonly, polyesters are obtained by direct polycondensation of dicarboxylic acids and diols using metal catalysts such as Lewis acids, rare earth triflates, and triflylimides. However, the removal of metal catalyst from polyesters is a tedious process and is a serious problem for the biological study of these polymers (24–26). Recently, Takai and coworkers developed a new method to synthesize polyesters employing the catalyst bis(nonafluorobutanesulfonyl)imide (NF_2NH) which can be removed by either simple washing or sublimation from the reaction flask during the reaction (27).

Calcium phosphates (CaP) are an excellent candidate for the inorganic phase because of their bioactivity and similar composition to natural bone (10). It has been reported that calcium and phosphate ions released by CaP dissolution can act as simple signaling molecules that are capable of inducing progenitor and stem cell differentiation (28). When cells are exposed to appropriate ion concentrations, their cell cycle progression is modulated resulting in proliferation. Also, sufficient Ca^{2+} and PO_4^{3-} release is hypothesized to upregulate the expression of some of the osteogenic genes such as osteocalcin (OCN) and osteopontin (OPN), which are known to regulate the extracellular matrix mineralization. Calcium and phosphate ion release can also induce the secretion of bone morphogenesis protein 2 (BMP-2) and activate BMP signaling pathways necessary for bone formation (29–31). Thus, the challenge in using calcium phosphates, for the inorganic phase of bone substitutes, is to regulate the calcium and phosphate ion release rate over time which is dependent on different parameters such as nanocrystallinity and Ca/P ratio (32). The ratio of Ca/P is one of the most important parameters that affects the material properties of different calcium phosphates and ranges from as high as 1.67 (hydroxyapatite) and as low as 0.5 (monobasic calcium phosphate-MCP). In general, the lower the Ca/P ratio is, the greater the solubility of the material and acidity of the resulting solution (33).

In this report, polyester/ceramic composites were fabricated and characterized for their potential to be utilized for bone regenerative engineering applications. Specifically, six novel polyesters were synthesized and their degradation behavior and inherent bioactivity assessed.

These polyesters were then composited with MCP to determine their complementary impact on ion release and osteoinductivity.

MATERIALS AND METHODS

Polymer Synthesis

NF_2NH was purchased from Alfa Chemistry. Succinic acid, glutaric acid, adipic acid, 1,5-pentanediol, and 1,8-octanediol were purchased from Sigma-Aldrich. The general procedure for achieving polycondensation polymerization for the synthesis of polyesters was modified from a previously published method (27) and is detailed below. In an oven-dried 500 mL round bottom flask glutaric acid (10.0 g, 75 mmol), 1,5-pentanediol (7.882 g, 75 mmol), and NF_2NH (43 mg, 0.075 mmol) were added and stirred by magnetic stir bar at 80 °C until the reaction mixture became homogeneous. Once well mixed, the vessel pressure was gradually decreased from ambient to 0.03 mmHg and the reaction was allowed to proceed for up to 30 h. After 30 h, a white solid was obtained in 84% yield (18.13 g) as calculated by the following relationship:

$$\text{yield}(\%) = \frac{W_{\text{reaction}}}{W_{\text{diacid}} + W_{\text{diol}} + W_{\text{catalyst}}} \times 100$$

where W_{reaction} , W_{diacid} , W_{diol} , and W_{catalyst} are obtained weight, diacid weight, diol weight, and catalyst weight, respectively. A summary of the polymers synthesized is provided in Table I.

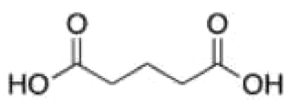
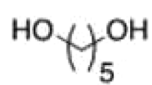
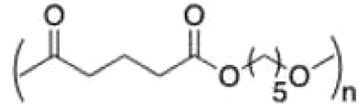
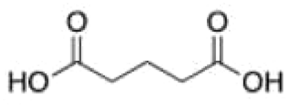
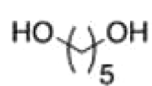
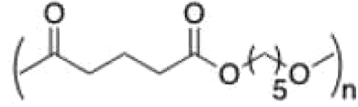
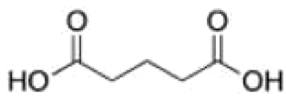
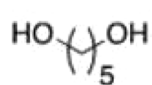
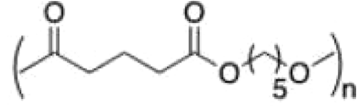
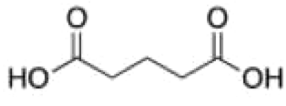
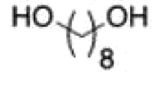
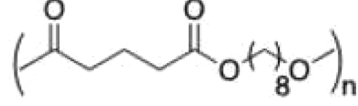
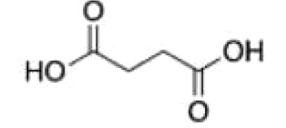
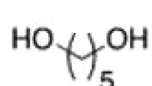
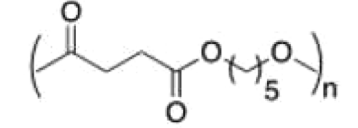
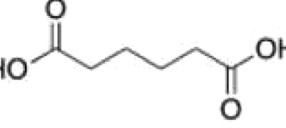
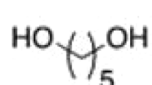
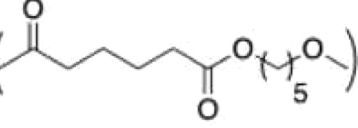
Polymer Characterization

Polymer chemical composition was evaluated with nuclear magnetic resonance. Proton NMR (^1H) spectra were recorded, using deuterated chloroform (CDCl_3) as the solvent, on either a Bruker DRX-300 (300 MHz), an AVIII-500 (500 MHz), or an AVIII-600 (600 MHz) spectrometer with chemical shifts reported in δ ppm with tetramethylsilane as an internal reference. Carbon NMR (^{13}C) spectra were obtained on the same instruments at 75, 125, and 150 MHz, respectively, in CDCl_3 solvent with CDCl_3 (77.0 ppm) as an internal reference.

Fourier transform infrared (FTIR) spectra were recorded on Nicolet 6700 FTIR (Thermo Scientific). Spectra were obtained in the range of 4000 to 400 cm^{-1} with the purpose of evaluating the chemical structure, especially ester bonds in the end-products.

The extent of polymerization was measured by a Hewlett Packard 1050 gel permeation chromatography (GPC) system equipped with a Polymer Sciences PL-ELS 1000 evaporative light scattering detector and a Waters Styragel HR-3 GPC column (4.6 × 300 mm). Samples were dissolved in chromatographic grade tetrahydrofuran (THF) at 10 mg/mL and run at 25 °C with a THF flow rate of 0.25 mL/min. Number average molecular weight (M_n), weight average molecular weight (M_w), and polydispersity index (PDI) were determined by comparing data against calibration curves prepared using polystyrene standards of 2.5, 5.0, 9.0, 17.5 k, and 30 k M_w .

Table I. Synthesis procedure, monomer and polymer structure, and naming convention

Diacid + Diol + $Nf_2NH \xrightarrow[0.03 \text{ mmHg}, 30 \text{ h}]{80 \text{ }^\circ\text{C}}$ Polyester				
Diacid	Diol	Time	Polyester	Abbreviation
		6 h		GlirPentE ₆
		16 h		GlirPentE ₁₆
		30 h		GlirPentE ₃₀
		30 h		GlirOctE ₃₀
		30 h		SucPentE ₃₀
		30 h		AdPentE ₃₀

The thermal properties of the polyesters were assessed using a modulated differential scanning calorimeter (TA-Q2000 V24.9 Build 121 thermal analyzer and the Universal V4.5A TA instruments). The ramp method was utilized employing a heat rate of 5 °C/min up to 120 °C. The melting temperature was calculated for each polymer.

Water contact angle (WCA) of the polyesters were measured by the sessile drop method, using a standard contact angle goniometer (Rame-Hart model 200). DROPimage Standard software was utilized to calculate the contact angle of each polymer.

Polymer Degradation Study

Polymer degradation studies were carried out in distilled, deionized water (ddH₂O) at room temperature for a period of 1 month. Change in Mw and Mn were measured after 14 and 28 days of degradation. Also, at specific time intervals (1, 2, 3, 7, 14, 21, and 28 days), the samples were removed, air-dried at room temperature, and assessed for weight loss using the following relationship (34):

$$W_{\text{loss}} \% = \frac{w_0 - w_t}{w_0} \times 100\%$$

where w_0 is the initial weight of the sample before immersion and w_t is the sample weight at a specific time point. The ddH₂O was exchanged at each time point and the solution pH and turbidity were recorded. The results reported are an average of three independent measurements.

Composite Sample Preparation and Characterization

Polyester/MCP composites were fabricated by the following solvent casting method (35). Each polyester was dissolved in chloroform after which MCP powder (Jost Chemical Company) was suspended in the polymer solution at a 70/30 polymer/ceramic ratio (36). Samples were treated by ultrasonication until MCP was well dispersed in the solution, mixed for 2 h at room temperature, and then the solutions were cast into a mold. The solvent was allowed to evaporate for 24 h under ambient conditions after which they

were further dried under vacuum for 36 h. The chemical structure of the composites were evaluated by FTIR and compared with the polyesters and MCP individually (spectra are available in supplementary data—Fig. S14—Fig. S20).

Composite Ion Release Study

Phosphate and calcium ion release from the composites and MCP alone was measured in ddH₂O at room temperature over 14 days. The composite films were immersed in ddH₂O and MCP powder was placed in a Transwell insert (Corning) then immersed in water. At certain time points, ddH₂O was exchanged and the solution was saved for ion release measurements.

Calcium release was measured using the Calcium LiquiColor assay (Stanbio laboratory) following the manufacturer's protocol. In brief, the solution were diluted by a color and base reagent, mixed well, and read by a multi-well plate reader (BioTek Cytation 5) at 550 nm. The absorbance was converted to calcium ion content using a standard concentration curve in the linear range (0–15 mg/dL). Samples above the linear range were diluted with ddH₂O prior to mixing with color and base reagents.

Phosphate release was measured using the phosphate colorimetric assay kit (Sigma-Aldrich) according to the manufacturer's procedure. In brief, the samples were mixed with phosphate reagent in a horizontal shaker and incubated at room temperature protected from light for 1 h. The absorbance was recorded at 650 nm with the plate reader. The absorbance was converted to phosphate ion content using a standard curve in the linear range (0–5 nmol). Samples above the linear range were diluted with ddH₂O prior to mixing with reagent.

Cell Culture and Seeding

Mesenchymal stem cells (MSCs) were purchased from Cyagen. The MSCs were initially cultured in T-75 cell culture flasks (Corning) and grown in Dulbecco's modified Eagle's medium (DMEM, Invitrogen) supplemented with 10% fetal bovine serum (FBS, Invitrogen) and 1% Penicillin-streptomycin (Pen-Strep, Invitrogen) at 37 °C in a humidified incubator with 5% CO₂. Media was changed every 48 h until cells approached confluency (~80%) when they were dissociated using a 0.05% trypsin-EDTA (Invitrogen) solution, counted by hemocytometer, and passed to new T-75 flasks at a splitting ratio of 1:4 or 1:5. After the fifth passage, cells were used for *in vitro* bioactivity studies. Solvent cast films (2 mm × 5 mm) comprised of polyester or 70/30 polyester/MCP were placed into 24-well plates and seeded with 30,000 cells/well. Tissue cultured polystyrene was seeded with 30,000 cells/well and exposed to MCP loaded in a Transwell insert or media alone as controls. MSCs were cultured for up to 14 days at 37 °C in a humidified incubator with 5% CO₂ and FBS and Pen-Strep supplemented DMEM media was changed every 72 h. Cellular proliferation, viability, alkaline phosphatase (ALP) activity, and mineralization were assessed at 1, 3, 7, and 14 days.

Proliferation Assay

Cellular proliferation was determined by the Quanti-iT PicoGreen dsDNA assay (Thermo Fisher Scientific). At each

endpoint, the films were rinsed with PBS and exposed to Triton X-100 (Sigma-Aldrich) followed by three freeze-thaw cycles in order to lyse the cells. Lysates were diluted by TE buffer (200 mM Tris-HCL, 20 mM EDTA, pH 7.5) and mixed with PicoGreen reagent according to the manufacturer's protocol. A plate reader was utilized to measure the fluorescence of each sample (e.g., 480 nm/em. 520 nm) and cell number was calculated using a MSC standard curve (0–200,000 cells).

Viability Assay

Cell viability was evaluated at each time point using a MTS cell proliferation colorimetric assay kit (BioVision). MTS reagent was added to media (20 µL per 200 mL media) followed by 4 h incubation at 37 °C in a humidified incubator with 5% CO₂. Absorbance of each sample was measured at 490 nm. Cell viability was normalized by cell count and reported as the ratio of absorbance in the samples compared to the negative control.

Alkaline Phosphatase Activity Assay

ALP activity of the MSCs exposed to the different biomaterials was quantified at each time point using an alkaline phosphatase assay kit (BioVision). In brief, 20 µL of cell lysate was combined with 50 µL of p-nitrophenyl phosphate (pNPP) in assay buffer. The mixture was incubated for 1 h at room temperature while kept away from light. The reaction was stopped by adding 20 µL of the stop solution and the absorbance of the solution at 405 nm was measured with a plate reader. To eliminate the effect of background, 1% Triton X-100 was incubated with pNPP, exposed to stop solution in assay buffer after 1 h, and its absorbance deducted from sample absorbance. The absorbance was converted to content of dephosphorylated p-nitrophenyl (pNP) using a pNP standard curve (0–20 nmol) which was dephosphorylated using excess ALP enzyme. ALP activity was reported as the pNP content normalized by cell count.

Mineralization Assay

Cell-based mineral deposition was measured at each time point using an alizarin red assay. At each time point, media was removed, the contents were washed by ddH₂O, and the sample was fixed in 70% ethanol for 24 h. The ethanol was removed and the samples were incubated in 1 mL of 40 mM alizarin red solution (Sigma-Aldrich) for 10 min. The samples were rinsed with ddH₂O several times to make sure all non-absorbed stain was removed. Absorbed alizarin red was desorbed using 1 mL of a 10% cetylpyridinium chloride (CPC, Sigma-Aldrich) solution and stain concentration was measured at 550 nm using a plate reader. Absorbance of each sample was converted to the concentration of absorbed alizarin red by a standard curve in linear range (0–0.2740 mg/mL). Samples above the linear range were diluted with CPC. Cell-based mineral deposition was calculated by subtracting mineralization induced by acellular films exposed to the same experimental conditions. All results were normalized by cell count.

Statistical Analysis

JMP software was used to make comparisons between groups using Tukey's HSD test to determine parallel statistical differences ($p < 0.05$). Within the figure graphs, groups that possess different letters have statistically significant differences in mean whereas those that possess the same letter are statistically similar.

RESULTS

Polyester Chemical Structure and Thermal Properties

^1H and ^{13}C NMR spectra were recorded as follows. The spectra are shown in the supplementary data (Fig. S1–Fig. S8). GlrPentE: ^1H NMR (500 MHz, CDCl_3) δ 4.07 (*t*, $J = 6.5$ Hz, 4H), 2.37 (*t*, $J = 7.5$ Hz, 4H), 1.94 (Pentet, $J = 7.5$ Hz, 2H), 1.65 (Pentet, $J = 7.0$ Hz, 4H), 1.44–1.38 (m, 2H); ^{13}C NMR (125 MHz, CDCl_3) δ 172.9, 64.1, 33.2, 28.2, 22.3, 20.1; GlrOctE: ^1H NMR (500 MHz, CDCl_3) δ 4.06 (*t*, $J = 6.5$ Hz, 4H), 2.36 (*t*, $J = 7.5$ Hz, 4H), 1.94 (Pentet, $J = 7.5$ Hz, 2H), 1.62–1.58 (m, 4H), 1.32 (s, 8H); ^{13}C NMR (125 MHz, CDCl_3) δ 172.9, 64.2, 33.3, 29.0, 28.5, 25.7, 20.1; SucPentE: ^1H NMR (500 MHz, CDCl_3) δ 4.09 (*t*, $J = 6.5$ Hz, 4H), 2.62 (s, 4H), 1.66 (Pentet, $J = 6.5$ Hz, 4H), 1.44–1.38 (m, 2H); ^{13}C NMR (125 MHz, CDCl_3) δ 172.3, 64.4, 29.0, 28.1, 22.3; AdPentE: ^1H NMR (500 MHz, CDCl_3) δ 4.08 (*t*, $J = 6.5$ Hz, 4H), 2.33 (*t*, $J = 6.0$ Hz, 4H), 1.67 (Pentet, $J = 7.5$ Hz, 8H), 1.45–1.39 (m, 2H); ^{13}C NMR (125 MHz, CDCl_3) δ 173.3, 64.1, 33.8, 28.2, 24.3, 22.3.

The FTIR spectra of the polymers were used to confirm the presence of ester bonds in the polymer backbone. The strong absorption bands at 1172 and 1719 cm^{-1} for GlrPentE, 1162 and 1727 cm^{-1} for GlrOctE, 1153 and 1726 cm^{-1} for SucPentE, and 1162 and 1724 cm^{-1} for AdPentE observed in the FTIR spectra showed the ester bonds in the polymers. The FTIR spectra are provided in Fig. S10–Fig. S13.

The molecular weight, appearance, yield, melting point, and water contact angle of the polyesters are reported in Table II. A sample DSC spectra can be found in Fig. S9. As shown in the table, increasing reaction times for GlrPentE polymers yielded a dramatic increase in degree of polymerization as well as heat of fusion and melting point. Increasing diol monomer length (GlrOctE30) or altering diacid monomer length (SucPentE30 and AdPentE30) did not impact the degree of polymerization but did decrease the melting point indicating that the symmetrical structure of GlrPentE30 compared to the other polyesters influences thermal properties. Molecular weight and chemistry both had an influence on hydrophilicity of the polymers. GlrPentE30 possessed a higher WCA compared to GlrPentE6 and GlrPentE16 which was due to increased chain length. GlrOctE30 and AdPentE30 had the highest WCA among all polyesters indicating the hydrophobic behavior of these polyesters which can be explained by the increased monomer hydrocarbon content.

Polymer Erosion and Degradation

Mass loss and molecular weight changes of the polyesters over 28 days is illustrated in Fig. 1. As shown in Fig. 1a, the

speed and extent of mass loss is dependent on polymer length with shorter polymers undergoing quicker and more significant mass loss over time (GlrPentE6 > GlrPentE16 > GlrPentE30). The degradation rate and subsequent decrease in molecular weight (Fig. 1c) was found to follow a reverse trend (GlrPentE6 < GlrPentE16 < GlrPentE30) and all polymers possessed similar molecular weights after 28 days. Erosion and degradation differences caused by polyester chemistry were found to be more complex. Monomer length was found to directly correlate to the rate of erosion with increasing length yielding slower and less significant erosion (SucPentE30 < AdPentE30~GlrPentE30 < GlrOctE30) over time (Fig. 1b). Interestingly, while SucPentE30, AdPentE30, and GlrOctE30 all possessed degradation profiles relative to their mass loss profiles (Fig. 1d), GlrPentE30 was found to undergo the most rapid and significant degradation over 28 days.

Solution pH change due to polyester degradation over 28 days is illustrated in Fig. 2 and was found to never drop below 3.5 for any of the samples. While pH drop magnitude followed a trend of decreasing polymer length during the first day, all other time points reveal very similar solution pH (Fig. 2a). For monomer chemistry (Fig. 2b), GlrPentE30 was found to induce the quickest solution pH drop though SucPentE30 yielded a similar pH drop at later time points (21 and 28 days). AdPentE30 and GlrOctE30 were responsible for more moderate pH changes. For all of the polyesters, the change in turbidity of solution containing the erosion and degradation products was found to be negligible (data not shown). Therefore, the degradation products are water soluble and not forming aggregates in ddH₂O indicating that they could be easily eliminated from an implantation site.

Ion Release Study

Calcium and phosphate ion release profiles for each composite and monobasic calcium phosphate are reported in Fig. 3, respectively. MCP is a highly water soluble powder which undergoes a quick burst of calcium and phosphate ion release reaching plateaus within 2–3 days. Polymer length was found to be quite important in composite ion release as lower molecular weight polyesters (GlrPentE6 and GlrPentE16) were found to possess similar ion release profiles to MCP alone whereas the higher molecular weight polyester (GlrPentE30) yielded slower and more controlled ion release profiles (Fig. 3a and Fig. 3c). In contrast to mass loss and degradation rate, faster ion release was seen with AdPentE30 and GlrOctE30 than was observed for SucPentE30 and GlrPentE30 (Fig. 3b and Fig. 3d).

Solution pH changes due to the dissolution of composites and MCP are reported in Fig. 4. Interestingly, MCP induces a significant solution pH drop down to ~2.5 which moderates over 14 days recovering to ~6. Within the composites, this behavior and polyester degradation will dictate local pH drop. Polymer length plays a significant role in pH drop with lower molecular weight polyesters (GlrPentE6 and GlrPentE16) maintaining a rather acidic solution pH (~3) for the entirety of the study whereas higher molecular weight polyester (GlrPentE30) had its pH moderate to ~4.8 over 14 days (Fig. 4a). Monomer chemistry played less of a role in altering the pH change

Table II. Polymer Molecular Weights and Thermal Properties

Polymer name	Mw (103 g/mol)	Mn (103 g/mol)	M w / Mn	Yield (%)	Appearance	Melting point (°C)	Water contact angle (°)
GlrPentE6	7.5	4.2	1.78	76	Colorless oil	20.6	33.1
GlrPentE16	14.4	13.2	1.43	85	White solid	23.0	37.0
GlrPentE30	21.1	13.1	1.61	84	White solid	48.6	68.5
GlrOctE30	24.2	17.1	1.41	87	White solid	22.0	91.3
SucPentE30	18.6	13.1	1.42	84	Colorless oil	19.2	67.6
AdPentE30	21.0	14.6	1.44	86	White solid	23.0	89.1

initially and over longer periods of time though GlrPentE30 was found to maintain a lower solution pH for days 3–5 (Fig. 4b).

Polymer/Ceramic Composite Cytotoxicity

The impact of cell proliferation on MSCs exposed to polyester films and polyester/MCP composite films over 14 days is shown in Fig. 5. MSCs seeded on tissue cultured plastic (Ctrl) and supplied growth media increased to a statistically significant six times initial seeding and cells additionally exposed to MCP dissolution maintained counts similar to initial seeding. Polymer length significantly impacted MSC proliferation as cells exposed to lower molecular weight polyesters (GlrPentE6 and GlrPentE16) showed no change in proliferation whereas cells seeded on high molecular weight polyester (GlrPentE30) expanded to ~4 times initial seeding (Fig. 5a), a statistically significant increase. The inclusion of MCP with the lower molecular weight polyesters had no effect on MSC proliferation, but its inclusion with higher molecular weight polyester induced cells to increase to ~2 times initial seeding (Fig. 5a). Monomer chemistry did not significantly impact cell proliferation since GlrOctE30, SucPentE30, and AdPentE30 all showed relatively similar proliferation profiles as GlrPentE30 with and without MCP (Fig. 5b).

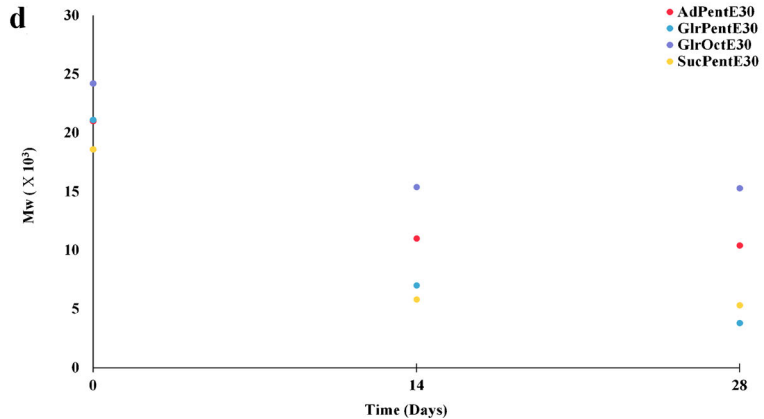
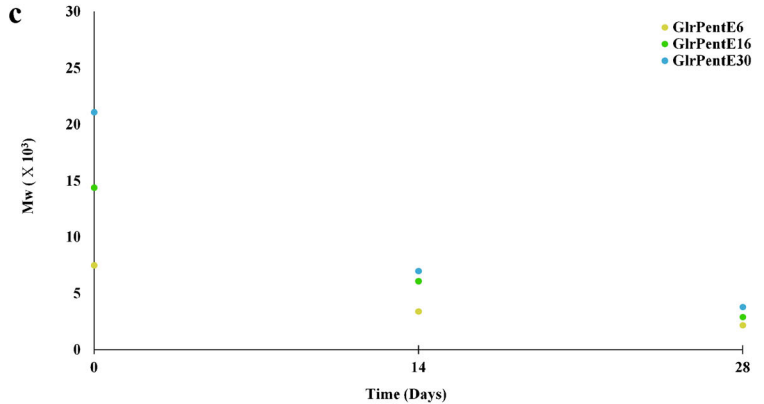
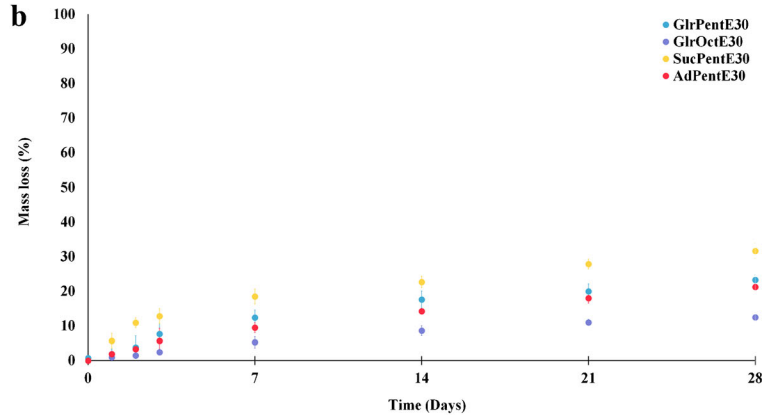
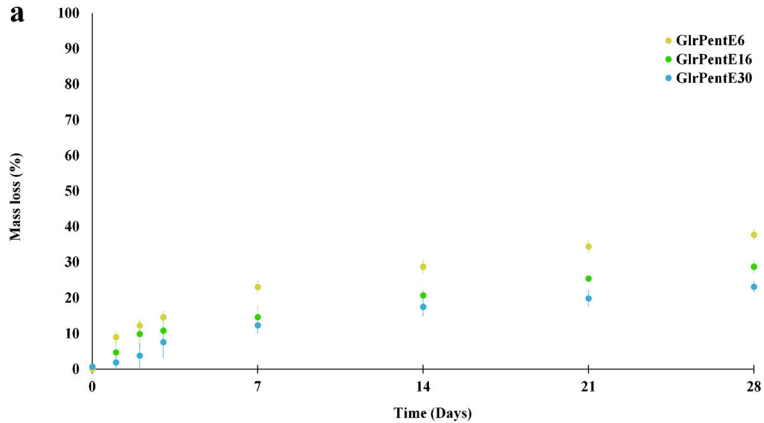
The viability of MSCs seeded on polyester films and polyester/MCP composite films over 14 days is detailed in Fig. 6. A MTS assay was used to measure metabolically active NAD(P)H-dependent dehydrogenase enzyme activity, an indirect measure of cell metabolism and viability. As shown in the graph, cell viability for cells grown on GlrPentE30/MCP, GlrOctE30/MCP, SucPentE30/MCP, and AdPentE30/MCP was significantly higher than their respective polymers, despite the fact that there were fewer cells on the composites as the experiment progressed. The increased metabolic activity of cells on the composites may be caused by the MSCs differentiating when exposed to composite films. The viability of MSCs exposed to MCP follows the same trend. After 14 days, the difference between the viability of cells cultured on the polymer film and MCP was statistically significant. GlrPentE6 and GlrPentE16 polymers and their composites, showed a higher level of cytotoxicity, which supports the theory that the fast degradation of these two polyesters and the subsequent rapid release of calcium and phosphate can cause sudden cell death.

Polymer/Ceramic Composite-Mediated *In Vitro* Stem Cell Differentiation

ALP activity of MSCs cultured on polyester films and polyester/MCP films over 14 days is overviewed in Fig. 7. MSCs exposed to the control conditions showed background levels of ALP expression while cells subjected to MCP dissolution showed a statistically significant increase in enzyme activity over time and compared to the control group. Polymer length significantly influenced ALP activity since cells exposed to lower molecular weight polyesters (GlrPentE6 and GlrPentE16) showed no ALP activity regardless of the absence or presence of MCP (Fig. 7a). In contrast, GlrPentE30/MCP composites induced significant ALP activity over time as well as greater than the MCP alone (Fig. 7a). Monomer chemistry also played a role in ALP activity with GlrOctE30/MCP and AdPentE30/MCP composites inducing similar cellular responses to MCP alone for all time points whereas GlrPentE30/MCP and SucPentE30/MCP composites achieved enhanced enzyme activity (Fig. 7b) over MCP alone.

Cell-based mineralization of MSCs due to contact with polyester films and polyester/MCP films over 14 days is described in Fig. 8. MSCs cultured under the control conditions showed minimal mineral deposition whereas those that interacted with MCP dissolution products deposited a statistically significant amount of mineral over time and compared to the control group. Figure 8a shows that polymer length dictated mineral deposition as composites with lower molecular weight polyesters (GlrPentE6/MCP and GlrPentE16/MCP) showed limited mineralization compared to statistically significant MSC-based mineralization seen with higher molecular weight polyester (GlrPentE30/MCP). Monomer chemistry played a role in the onset of mineralization with GlrOctE30/MCP and AdPentE30/MCP composites showing similar increases in deposition over time to MCP alone whereas GlrPentE30/MCP and SucPentE30/MCP induced more rapid increases in mineral deposition (Fig. 8b). By 14 days, the deposition rate was similar across all of these groups (Fig. 8b) and much higher than MCPs cultured under control conditions.

Fig. 1. Polyester mass loss and molecular weight loss over time. Mass loss was measured over 28 days and molecular weight changes were measured using GPC after 14 and 28 days in ddH₂O and room temperature for polyesters possessing **a, c** the same monomer structures and different molecular weights and **b, d** different monomer structure and similar molecular weights



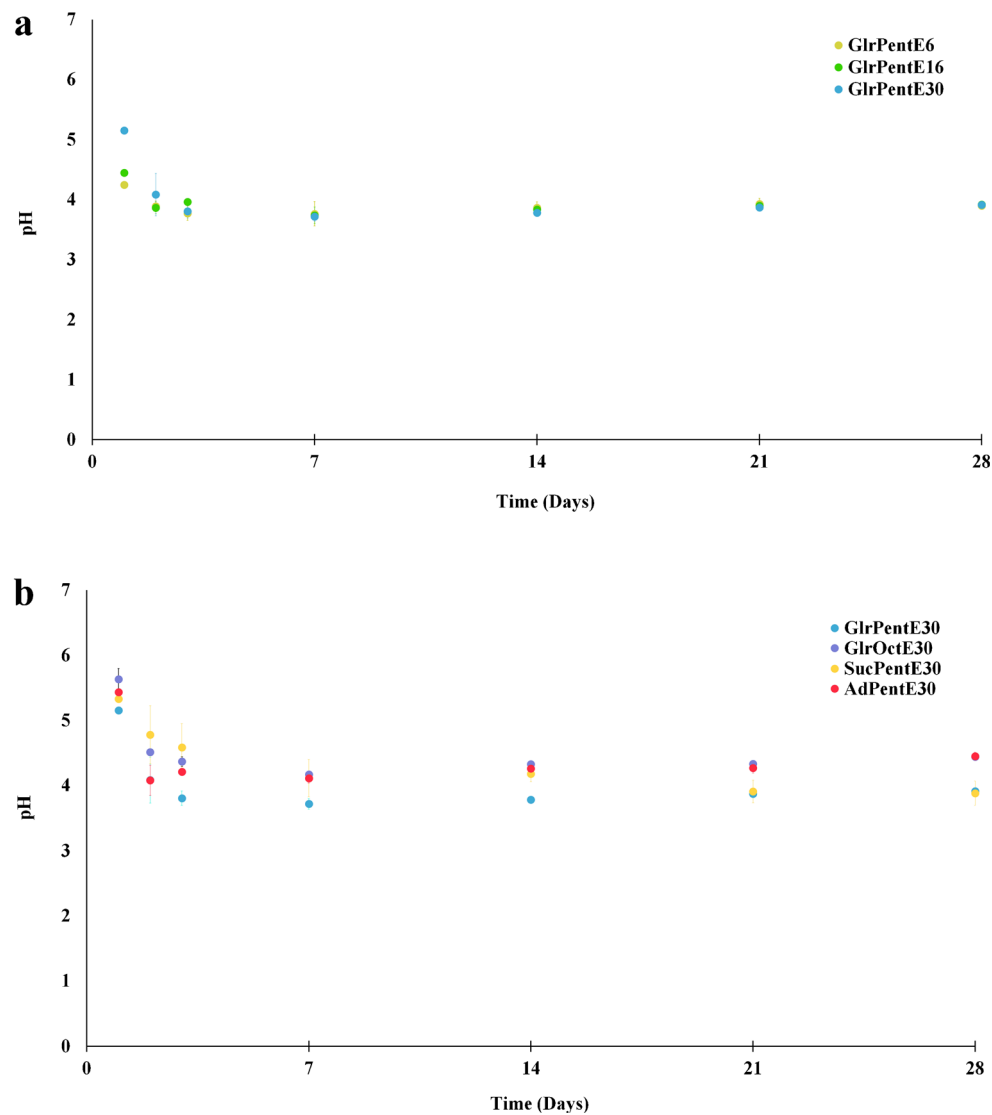


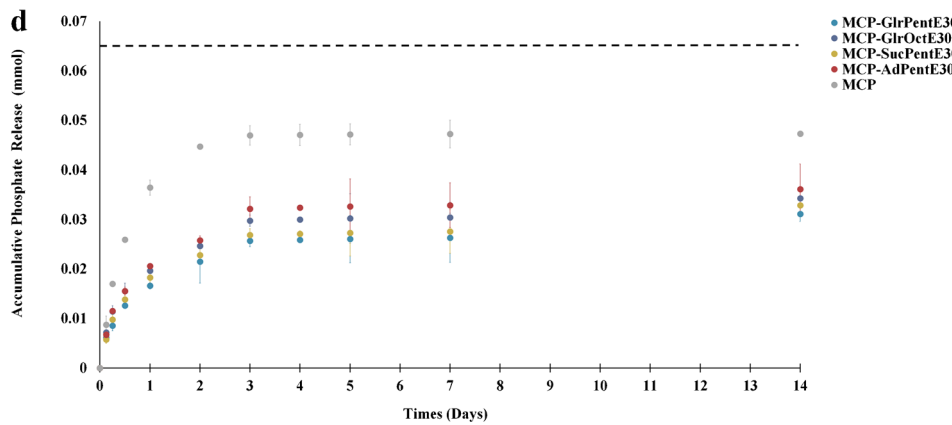
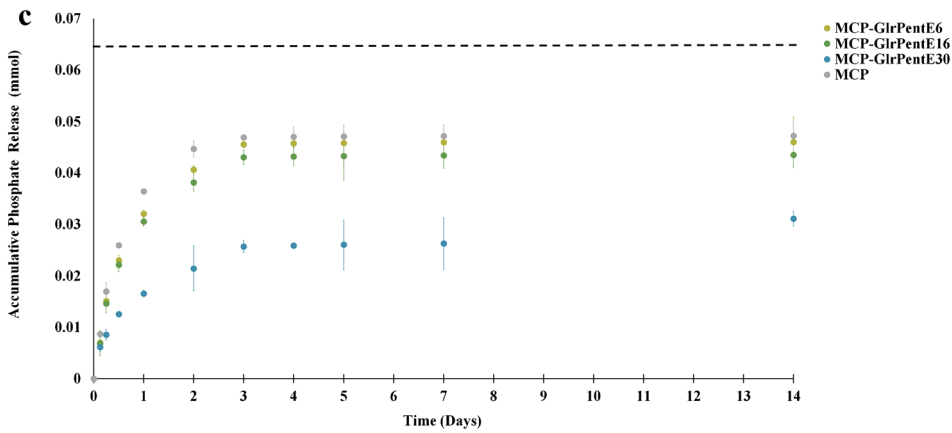
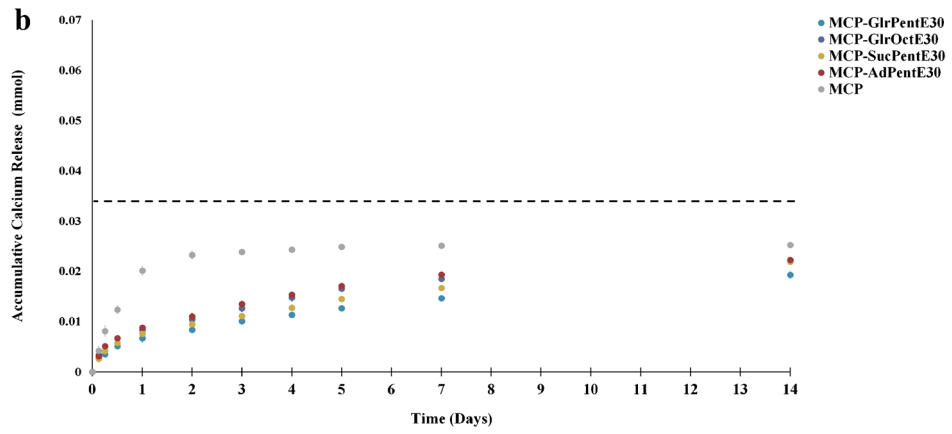
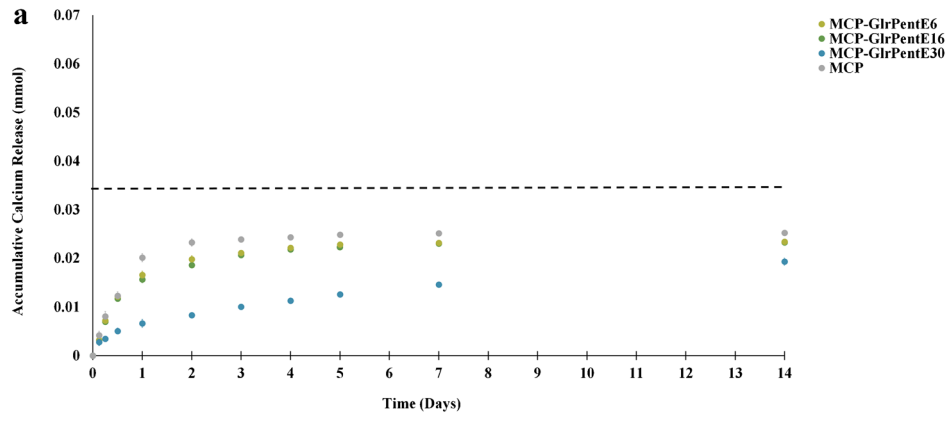
Fig. 2. Solution pH variation due to polyester erosion. Changes in pH were measured over 28 days of degradation in ddH₂O and room temperature for polyesters possessing **a** the same monomer structures and different molecular weights and **b** different monomer structure and similar molecular weights

DISCUSSION

In this decade, there has been an increasing interest in degradable material development for tissue engineering and regenerative medicine with polyesters with short aliphatic chains (i.e., polyglycolide and polylactide) being increasingly utilized. In this research, polyester structural changes were made and their impact on materials properties and potential for bone regenerative engineering applications investigated. Specifically, changes in polymer length and monomer length and symmetry were explored using GlrPentE as a reference polyester due to the unique hydrophilicity of its five-carbon monomer constituents. GlrPentE polymers of different molecular weights were synthesized by varying polymerization time (GlrPentE6, GlrPentE16, and GlrPentE30) and compared against polyesters with varying monomer lengths (GlrOctE30, SucPentE30, and AdPentE30). The degradation studies showed a drop in molecular weight along with detectable mass loss in all the polyesters over 1 month of

degradation under aqueous conditions. During the first 3 days of immersion, polyesters showed a higher rate of mass loss which indicates loss of the lower molecular weight chains into solution. Hydrolytically degradable polymers undergo a three-step erosion mechanism where water first infiltrates the polymer followed by bone hydrolysis yielding shorter polymers that are able to dissolve when they are small enough to be water soluble (37). The persistent but decreasing mass loss over time indicates that the novel polyesters synthesized for this research undergo bulk erosion similar to commonly utilized polyesters (38). Also, since polyester water

Fig. 3. Cumulative calcium and phosphate ion release. Concentration of calcium and phosphate ion was measured over 14 days of immersion in ddH₂O and room temperature for MCP alone and composites with polyesters possessing **a, c** the same monomer structures and different molecular weights and **b, d** different monomer structure and similar molecular weights. The dash line represented the maximum amount of calcium or phosphate ions possible based on the MCP embedded in the composite films



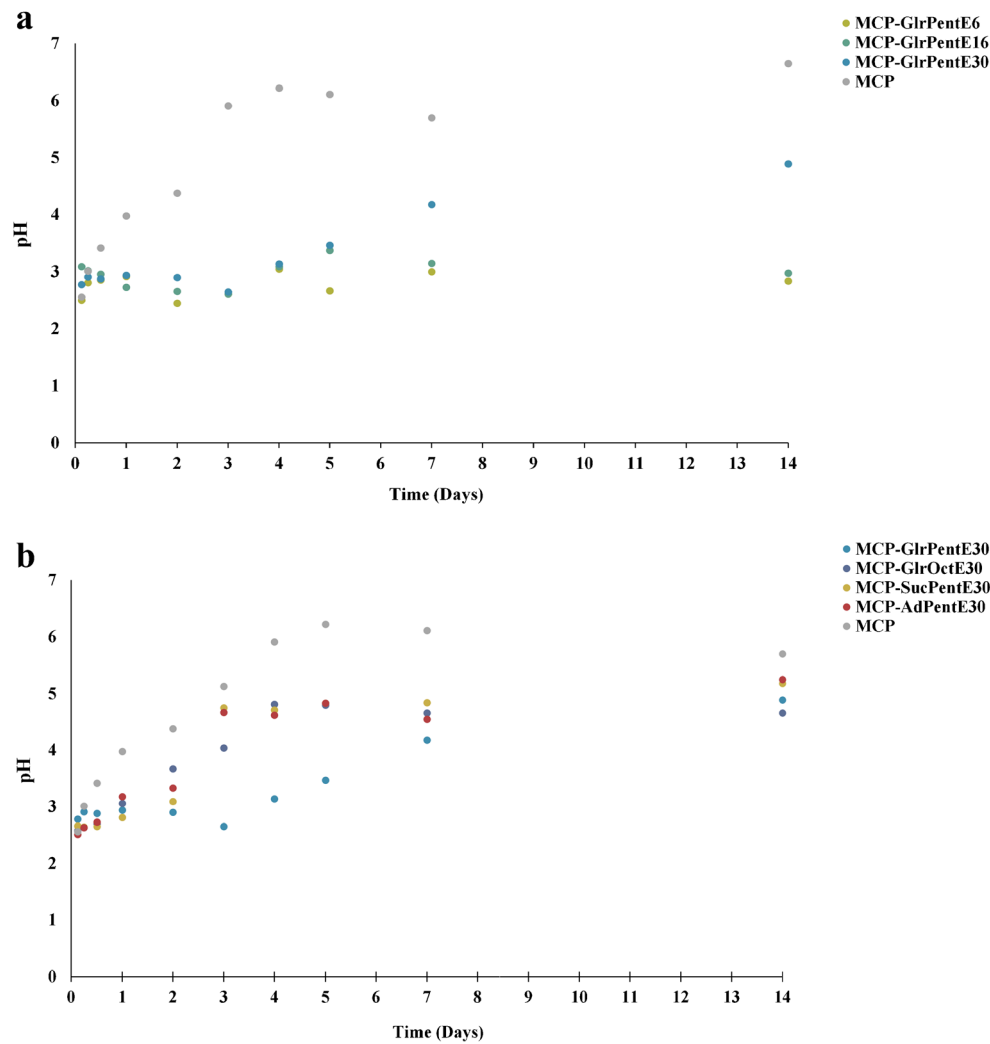


Fig. 4. Solution pH variation due to composite dissolution. Changes in pH was measured over 14 days of immersion in ddH₂O at room temperature for MCP alone and composites with polyesters possessing **a** the same monomer structures and different molecular weights and **b** different monomer structure and similar molecular weights

solubility and hydrophilicity decreases as polymer length increases, the relative mass loss of GlrPentE polymers (GlrPentE6 > GlrPentE16 > GlrPentE30) is related to the capacity of water to penetrate the polymer bulk. This trend is also seen when changing monomer chemistry where monomer water solubility and hydrophilicity (glutaric acid > succinic acid > adipic acid > 1,8-octanediol) is tied to mass loss and molecular weight changes. These results provide evidence that the degradation and erosion profiles of these novel polyesters can be readily tuned allowing for their use in a variety of regenerative engineering applications.

CaP is widely used in musculoskeletal tissue engineering scaffolds (35, 39–41). The major justification for its use has been its biomimicry of the inorganic phase of natural bone which contains hydroxyapatite and its inherent osteoinductivity (42, 43). Recent research has provided considerable insight into the mechanism dictating CaP osteoinductivity and results indicate it is the controlled release of calcium and phosphate ions from the ceramic that dictates its bioactivity (28, 31). For this research,

MCP, a rapidly dissolving CaP, was incorporated into the polyester matrices to investigate whether the polymers could control ion release thereby regulating MSC osteoblastic differentiation. Since MCP ion release and its related bioactivity are expected within the first 2 weeks of exposure, all composite characterization and cell studies were conducted for up to 14 days. MCP alone was found to rapidly dissociate releasing the majority of its ions within the first 2–3 days. MCP was the best candidate among commercially available calcium phosphates because it provides a rapid, transient delivery of ions. This property enabled the investigation of the ability of the polyesters to directly control release of ions. The polyester/MCP composites are able to function as a tunable system which can be optimized to deliver appropriate localized ion concentrations over time facilitating better cell proliferation and osteogenic differentiation. Low molecular weight polyesters (GlrPentE6 and GlrPentE16) were found unable to retard MCP ion dissolution whereas higher molecular weight polyester (GlrPentE30) was capable of controlling ion release for at least 14 days. Monomer chemistry also

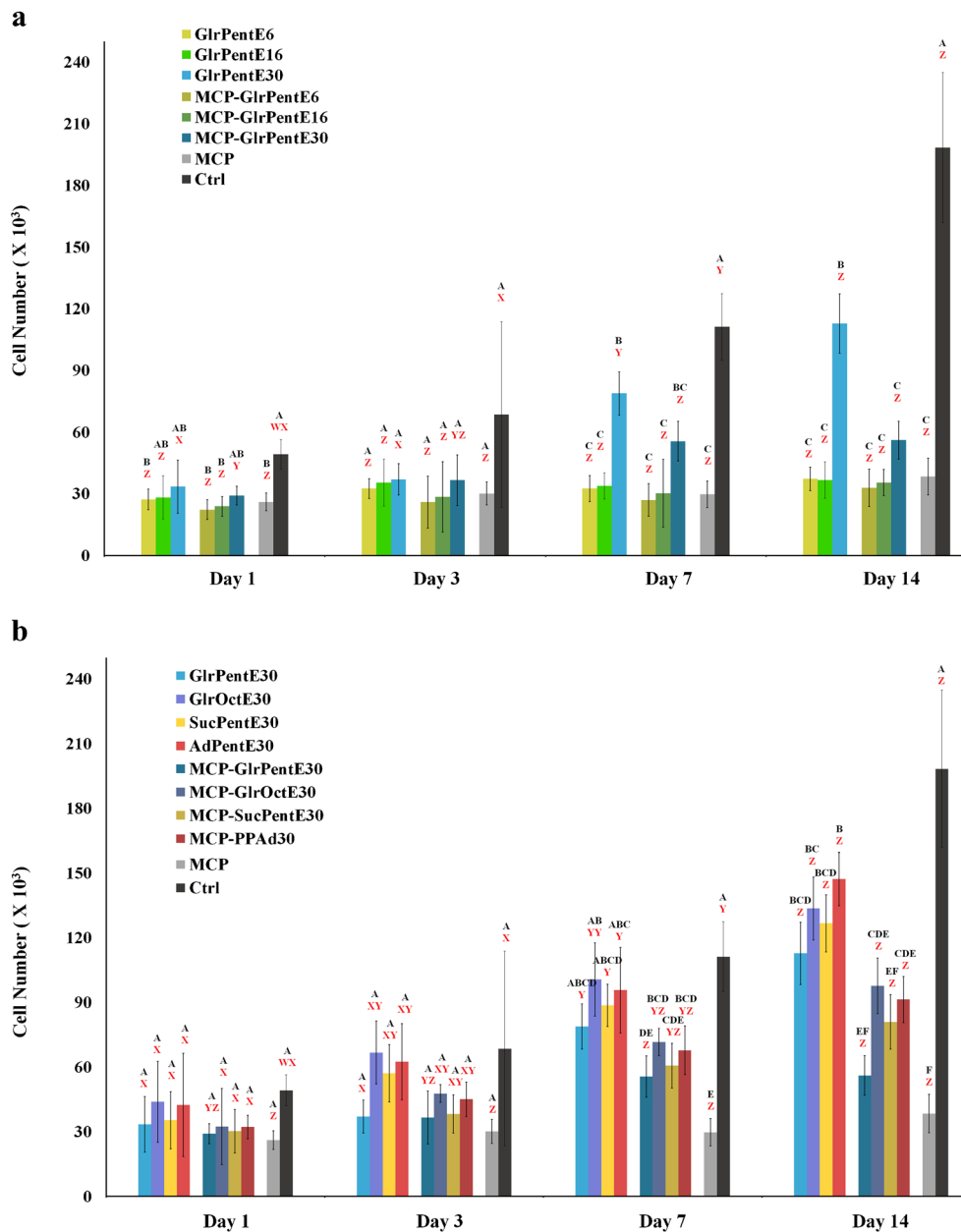


Fig. 5. Proliferation of MSCs cultured on polyester and polyester/MCP composites. Cell counts were measured by the Quanti-iT PicoGreen assay over 14 days of cell culture with polyester films and polyester/MCP composite films with **a** the same monomer structures and different molecular weights and **b** different monomer structure and similar molecular weights. Groups that possess different letters have statistically significant differences ($p < 0.005$) in mean whereas those that possess the same letter are statistically similar. *Black letters (A–F)* compare different material at the same time point while *red letters (W–Z)* compare specific materials over the four different time points

had some influence on MCP dissolution where faster eroding polyesters (GlrPentE30 and SucPentE30) achieved more controlled ion release compared to slower eroding polyesters (GlrOctE30 and AdPentE30). This observation suggests that calcium and phosphate ion release is not only dependent on matrix breakdown but also the more complex interactions between the CaP and polyesters phases. More hydrophobic GlrOctE30 and AdPentE30 slow the erosion profile of the material but also negatively impact the interaction between the polymer and CaP composite constituents during the film

deposition process. It is believed that the more hydrophilic GlrPentE30 and SucPentE30 are able to better distribute the MCP in the matrix allowing for more controlled release compared to the more hydrophobic polyesters. Embedding MCP into the polyester matrix was also able to modulate the local pH environment. Polyesters by themselves induced monomer dependent pH reduction to 3.5–4.5 over 7 days which remained stable for up to 28 days. MCP alone induced an immediate pH drop to 2.5 that moderated to 6–7 after 4 days. Composite materials showed that the presence of MCP was able to moderate

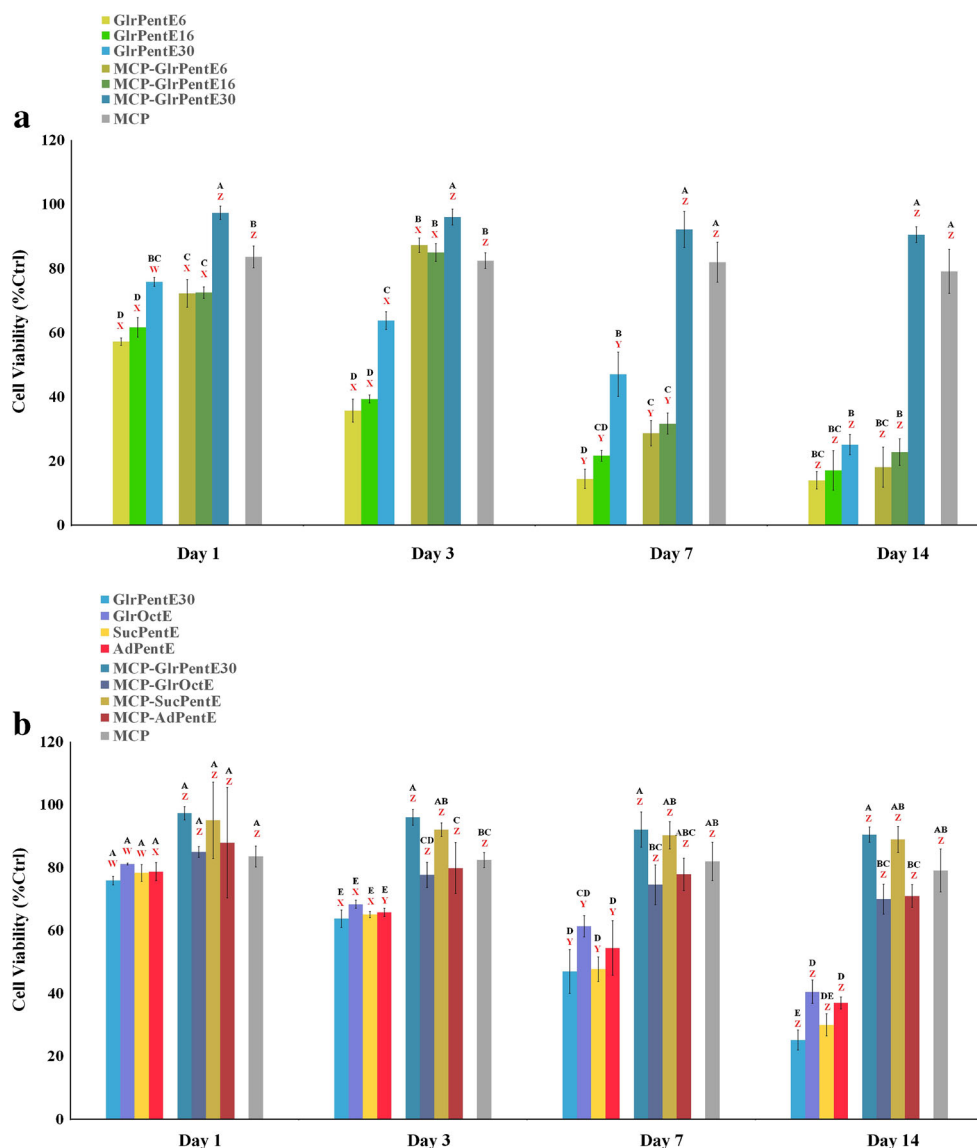


Fig. 6. Viability of MSCs cultured on polyester and polyester/MCP composites. NAD(P)H activity over 14 days was determined by an MTS assay and used as an indirect measure of cell metabolism and viability for MSCs exposure to polyester films and polyester/MCP composite films with **a** the same monomer structures and different molecular weights and **b** different monomer structure and similar molecular weights. Viability data were normalized on a per cell basis and then indexed to the Ctrl group. Groups that possess different letters have statistically significant differences ($p < 0.005$) in mean whereas those that possess the same letter are statistically similar. *Black letters (A–F)* compare different material at the same time point while *red letters (W–Z)* compare specific materials over the four different time points

the acidic pH of the high molecular weight polyester (GlrPentE30, GlrOctE30, SucPentE30, and AdPentE30) degradation products yielding pH values of 4.5–5.5 after 14 days. Comparatively, the pH of composites possessing lower molecular weight polyesters (GlrPentE6 and GlrPentE16) were unable to moderate polymer degradation product acidity and pH values of 2.5–3 were found after 14 days. These results suggest that the calcium and phosphate ions can buffer the aqueous environment but only when their release is controlled over time.

MSCs were exposed to different polyesters to investigate the effect of polymer length and monomer chemistry on cell proliferation and differentiation. Cells were also exposed to MCP and polyester/MCP composites to determine the impact of MCP incorporation on polymer matrix osteoinductivity.

MSCs exposed to lower molecular weight polymers (GlrPentE6 and GlrPentE16) and their composites (GlrPentE6/MCP and GlrPentE16/MCP) show no proliferation change over the experiment. This limited cell growth appears to be due to materials cytotoxicity since cell viability was found to be markedly decreased for MSCs seeded on these polymers. This behavior is believed to be tied to these materials yielded prolonged, highly acidic pH local microenvironments. In addition, decreased proliferation of MSCs exposed to GlrPentE6 and GlrPentE16 can be discussed in terms of these polymers being more hydrophilic than GlrPentE30. It is believed that if the surface is too hydrophilic proteins will not as readily adsorb to its surface consequently decreasing cell attachment and proliferation. MSCs exposed

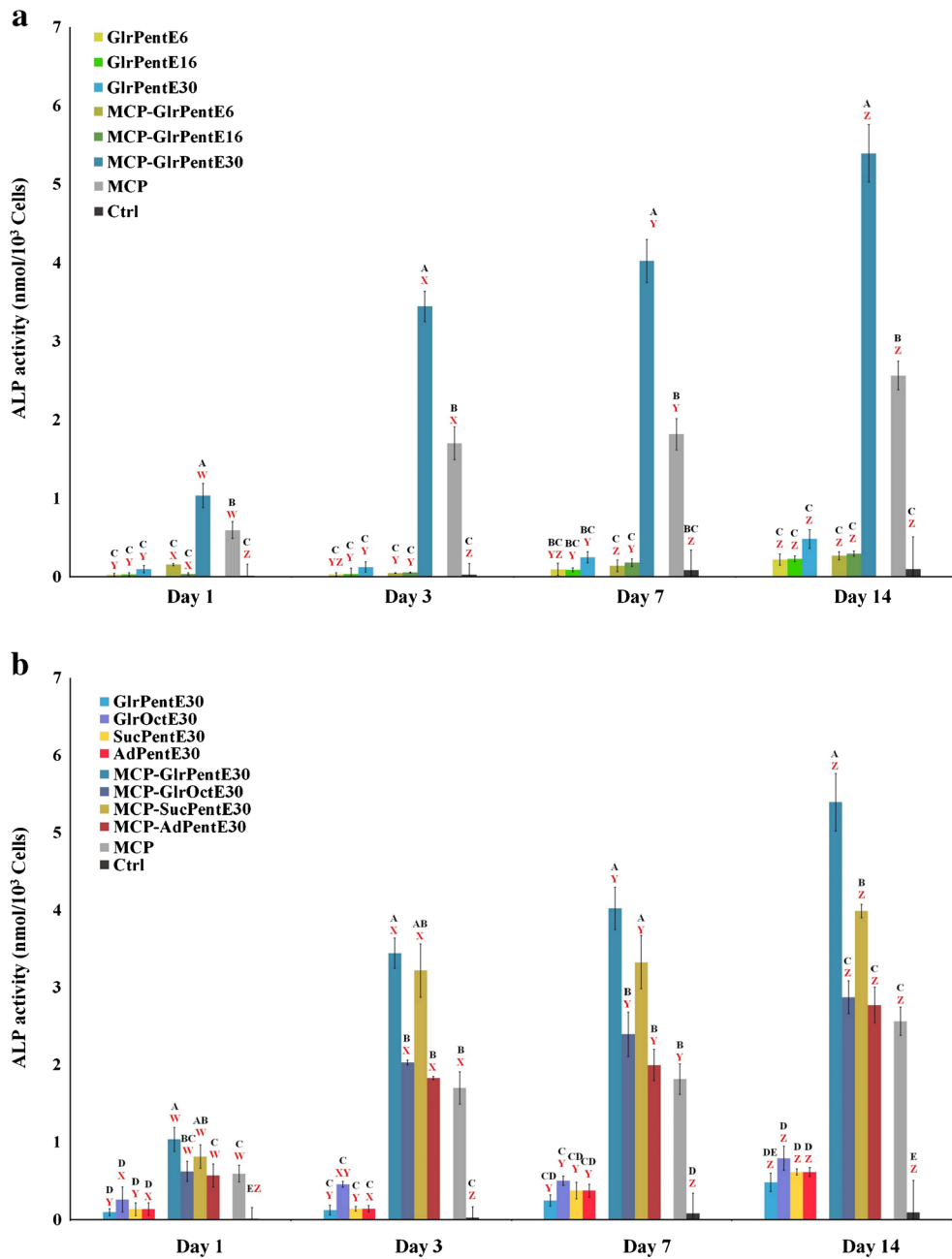


Fig. 7. ALP activity of MSCs cultured on polyester and polyester/MCP composites. Enzyme activity was analyzed by an alkaline phosphatase assay kit over 14 days of cell culture with polyester films and polyester/MCP composite films with **a** the same monomer structures and different molecular weights and **b** different monomer structure and similar molecular weights. ALP activity data were normalized on a per cell basis. Groups that possess different letters have statistically significant differences ($p < 0.005$) in mean whereas those that possess the same letter are statistically similar. *Black letters (A–F)* compare different material at the same time point while *red letters (W–Z)* compare specific materials over the four different time points

to higher molecular weight polyesters (GlrPentE30, GlrOctE30, SucPentE30, and AdPentE30) did not show statistically significant differences in proliferation from the control group over the first week but over time showed slightly reduced growth compared to control group. However, the viability of the cells exposed to these polyesters decreased significantly like due since pH changes can stress MSCs. Cells can respond to this stress in variety of ways ranging from the

activation of survival pathways to cell death (44). In this research, the MSCs were exposed to the local acidic environment associated with the degrading polyesters and their composites with MCP. The MTS assay was used to measure one enzyme activity (metabolically active NAD(P)H-dependent dehydrogenase enzyme). The result of MTS was reported as the ratio of this enzyme’s activity in MSCs growing in polyester acidic environment to those

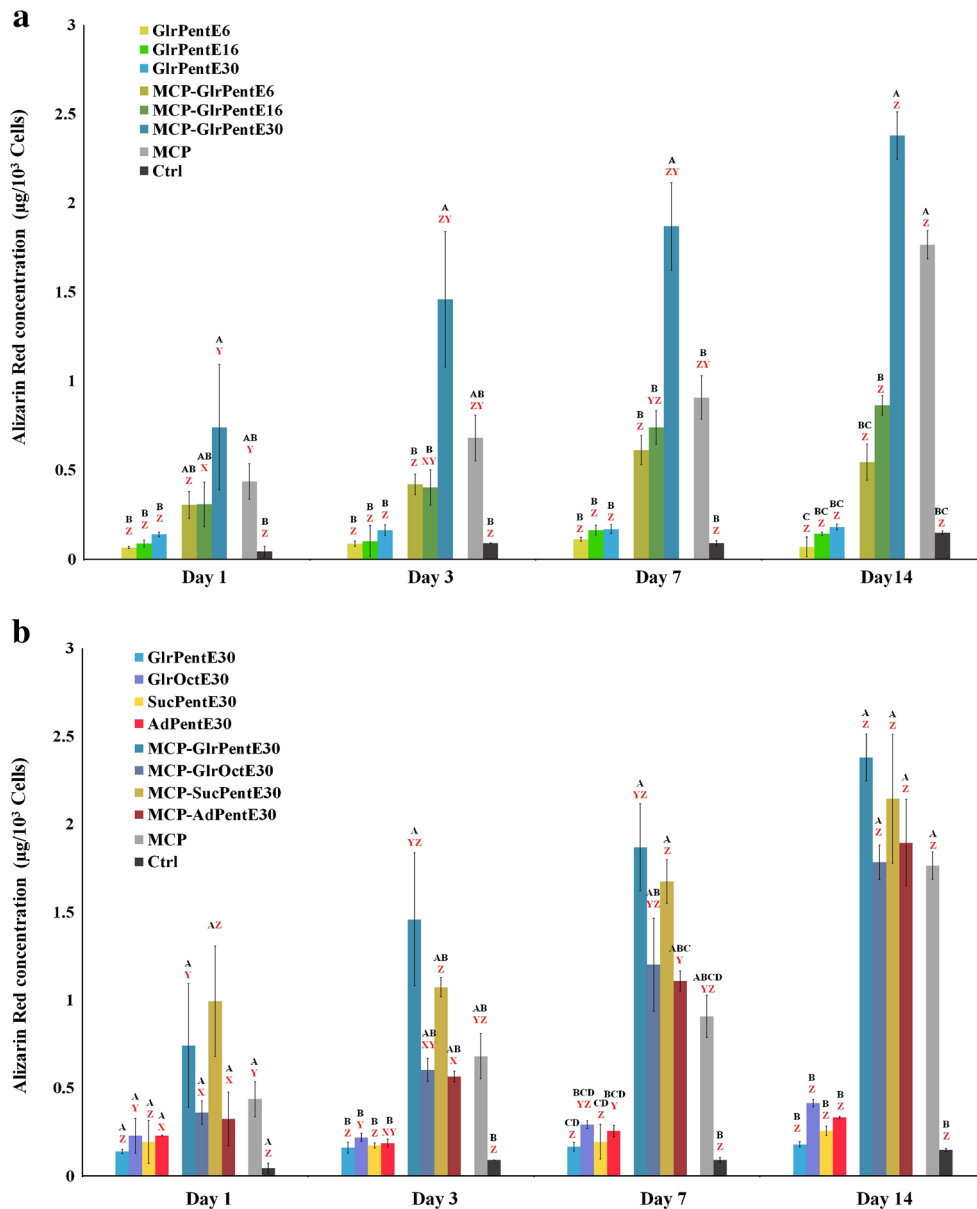


Fig. 8. Cell-based mineralization of MSCs cultured on polyester and polyester/MCP composites. Alizarin red staining was used as an indirect measure of mineralization over 14 days of cell culture with polyester films and polyester/MCP composite films with **a** the same monomer structures and different molecular weights and **b** different monomer structure and similar molecular weights. Mineralization data were normalized on a per cell basis. Groups that possess different letters have statistically significant differences ($p < 0.005$) in mean whereas those that possess the same letter are statistically similar. *Black letters (A–F)* compare different material at the same time point while *red letters (W–Z)* compare specific materials over the four different time points

growing in DMEM media (control group). The stressed cells were found to not have died but they showed diminished metabolic activity compared to rapidly dividing, unstressed, healthy MSC explaining why cell viability of the cells exposed to some materials dropped to less than 50%. MSCs exposed to high molecular weight polymer containing composites (GlrPentE30/MCP, GlrOctE30/MCP, SucPentE30/MCP, and AdPentE30/MCP) also showed statistically significant decreases in proliferation compared to the control group and their respective polymers alone at day 14. Reduced proliferation rate does not appear to be due to cytotoxicity

since viable cells were maintained through the experiment. This suggests that MSCs are likely differentiating and losing their capacity to divide. These results suggest that local pH and ion release play synergistic roles in influencing stem cell health and differentiation state.

To confirm that the MSCs exposed to high molecular weight polyester/MCP composites differentiated into osteoblasts, established bioactivity markers were assessed. ALP is an enzyme which is very active in bone and liver cells (45) and is considered an early marker of osteogenic differentiation. MSCs exposed to MCP or the high molecular weight

polymer containing composites (GlrPentE30/MCP, GlrOctE30/MCP, SucPentE30/MCP, and AdPentE30/MCP) showed statistically significant increases in ALP activity over controls and lower molecular weight polymer containing composites (GlrPentE6/MCP and GlrPentE16/MCP). Cell mineralization was also investigated since this is the hallmark functionality of a differentiated osteoblast. MSCs exposed to the same groups mentioned above were found to induce significantly greater quantities of deposited mineral than their respective polymers, the lower molecular weight polymer containing composites, and the media alone control. Interestingly, GlrPentE30/MCP and SucPentE30/MCP composites were found to induce greater ALP activity and more rapid onset of mineralization than GlrOctE30/MCP, AdPentE30/MCP, or MCP alone. This result coincides with the two polyesters that achieved modest improvements in prolonged calcium and phosphate ion release providing further evidence that CaP bioactivity is likely tied to controlled exposure of stem cells to these molecules.

The results indicate that the polyester/MCP composites have the potential to be optimized as a musculoskeletal substitute for enhanced osteoinductivity. The release of calcium and phosphate could lead to a combination of positive and negative consequences. Rapid ion release can dramatically decrease pH early on creating an unfavorable environment for cell growth and differentiation with high ion concentrations even being cytotoxic. On the other hand, sufficient concentration of these simple signaling molecules can activate desirable differentiation pathways and buffer pH changes. Therefore, the success of polymer/ceramic composites is highly dependent on the ion concentration and time course for which they are allowed to interact with MSCs. For future materials design, polymer chemistry and molecular weight as well as calcium phosphate content will need to be optimized to achieve the most desirable regenerative outcomes.

CONCLUSION

This research aimed to synthesize and characterize novel polyesters capable of incorporating rapidly dissolving monobasic calcium phosphate to create novel composite biomaterials for bone regenerative engineering. It was determined that polymer length, monomer chemistry, and ceramic entrapment greatly impacted materials properties especially the erosion rate, ion release rate, and local solution pH. Mesenchymal stem cells cultured on composite films were found to differentiate into mineral depositing osteoblasts for which bioactivity correlated to controlled ion release. The outcome of this research further supports that calcium and phosphate ions act as osteoinductive simple signaling molecules and controlling their release with a polymeric matrix is a promising approach for bone repair applications.

ACKNOWLEDGEMENTS

The authors gratefully acknowledge support from start-up funds provided by the University of Missouri. We also thank the Jost Chemical Company for providing

the monobasic calcium phosphate and specifically Jerry Jost, Doug Jost, and Joe Hardimon for valuable discussion regarding this research. AJG and BNA thank the Discovery Fellows Program at the University of Missouri for their support.

REFERENCES

1. Antonova E, Le TK, Burge R, Mershon J. Tibia shaft fractures: costly burden of nonunions. *BMC Musculoskelet Disord*. 2013;14(1):1.
2. Cross M, Smith E, Hoy D, Nolte S, Ackerman I, Fransen M, *et al*. The global burden of hip and knee osteoarthritis: estimates from the global burden of disease 2010 study. *Annals of the rheumatic diseases*. 2014;annrheumdis-2013-204763.
3. Feigin V. Global, regional, and national life expectancy, all-cause mortality, and cause-specific mortality for 249 causes of death, 1980-2015: a systematic analysis for the Global Burden of Disease Study 2015. *Lancet*. 2016;388(10053):1459-544.
4. Tataru AM, Mikos AG. Tissue engineering in orthopaedics. *J Bone Joint Surg Am*. 2016;98(13):1132-9.
5. Kainer MA, Linden JV, Whaley DN, Holmes HT, Jarvis WR, Jernigan DB, *et al*. Clostridium infections associated with musculoskeletal-tissue allografts. *N Engl J Med*. 2004;350(25):2564-71.
6. Xie C, Reynolds D, Awad H, Rubery PT, Pelled G, Gazit D, *et al*. Structural bone allograft combined with genetically engineered mesenchymal stem cells as a novel platform for bone tissue engineering. *Tissue Eng*. 2007;13(3):435-45.
7. Hutmacher DW. Scaffolds in tissue engineering bone and cartilage. *Biomaterials*. 2000;21(24):2529-43.
8. Benders KE, van Weeren PR, Badylak SF, Saris DB, Dhert WJ, Malda J. Extracellular matrix scaffolds for cartilage and bone regeneration. *Trends Biotechnol*. 2013;31(3):169-76.
9. Ravichandran R, Venugopal JR, Sundarajan S, Mukherjee S, Ramakrishna S. Precipitation of nanohydroxyapatite on PLLA/PBLG/collagen nanofibrous structures for the differentiation of adipose derived stem cells to osteogenic lineage. *Biomaterials*. 2012;33(3):846-55.
10. Liao S, Cui F, Zhang W, Feng Q. Hierarchically biomimetic bone scaffold materials: nano-HA/collagen/PLA composite. *J Biomed Mater Res B Appl Biomater*. 2004;69(2):158-65.
11. Agrawal C, Ray RB. Biodegradable polymeric scaffolds for musculoskeletal tissue engineering. *J Biomed Mater Res*. 2001;55(2):141-50.
12. Liu X, Ma PX. Polymeric scaffolds for bone tissue engineering. *Ann Biomed Eng*. 2004;32(3):477-86.
13. Kretlow JD, Mikos AG. Review: mineralization of synthetic polymer scaffolds for bone tissue engineering. *Tissue Eng*. 2007;13(5):927-38.
14. Shrivats AR, McDermott MC, Hollinger JO. Bone tissue engineering: state of the union. *Drug Discov Today*. 2014;19(6):781-6.
15. Vert M. Aliphatic polyesters: great degradable polymers that cannot do everything. *Biomacromolecules*. 2005;6(2):538-46.
16. Idris SB, Danmark S, Finne-Wistrand A, Arvidson K, Albertsson A-C, Bolstad AI, *et al*. Biocompatibility of polyester scaffolds with fibroblasts and osteoblast-like cells for bone tissue engineering. *J Bioact Compat Polym*. 2010;25(6):567-83.
17. Seyednejad H, Gawlitta D, Dhert WJ, van Nostrum CF, Vermonden T, Hennink WE. Preparation and characterization of a 3D-printed scaffold based on a functionalized polyester for bone tissue engineering application. *Functionalized Polyesters*. 2012;7(5):87.
18. Kanitkar A, Chen C, Smoak M, Hogan K, Scherr T, Aita G, *et al*. In vitro characterization of polyesters of aconitic acid, glycerol, and cinnamic acid for bone tissue engineering. *J Biomater Appl*. 2015;29(8):1075-85.

19. Ali Akbari Ghavimi S, Ebrahimzadeh MH, Solati-Hashjin M, Osman A, Azuan N. Polycaprolactone/starch composite: fabrication, structure, properties, and applications. *J Biomed Mater Res A*. 2015;103(7):2482–98.
20. Jiao Y-P, Cui F-Z. Surface modification of polyester biomaterials for tissue engineering. *Biomed Mater*. 2007;2(4):R24.
21. Carothers WH, Dorough G. Studies on polymerization and ring formation. IV. Ethylene succinates. *J Am Chem Soc*. 1930;52(2):711–21.
22. Jérôme C, Lecomte P. Recent advances in the synthesis of aliphatic polyesters by ring-opening polymerization. *Adv Drug Deliv Rev*. 2008;60(9):1056–76.
23. Robert C, de Montigny F, Thomas CM. Tandem synthesis of alternating polyesters from renewable resources. *Nat Commun*. 2011;2:586.
24. Ajioka M, Enomoto K, Suzuki K, Yamaguchi A. The basic properties of poly (lactic acid) produced by the direct condensation polymerization of lactic acid. *Journal of Environmental polymer degradation*. 1995;3(4):225–34.
25. Kobayashi S, Hachiya I, Yamanoi Y. Repeated use of the catalyst in Ln (OTf) 3-catalyzed aldol and allylation reactions. *Bull Chem Soc Jpn*. 1994;67(8):2342–4.
26. Ishihara K, Kubota M, Yamamoto H. A new scandium complex as an extremely active acylation catalyst. *Synlett*. 1996;1996(03):265–6.
27. Moyori T, Tang T, Takasu A. Dehydration polycondensation of dicarboxylic acids and diols using sublimating strong Brønsted acids. *Biomacromolecules*. 2012;13(5):1240–3.
28. Ulery BD, Nelson SJ, Deng M, Lo KW, Khan YM, Laurencin CT. Simple Signaling Molecules for Inductive Bone Regenerative Engineering. 2014.
29. Bolander J, Chai YC, Geris L, Schrooten J, Lambrechts D, Roberts SJ, et al. Early BMP, Wnt and Ca 2+/PKC pathway activation predicts the bone forming capacity of periosteal cells in combination with calcium phosphates. *Biomaterials*. 2016a;86:106–18.
30. Bolander J, Ji W, Geris L, Bloemen V, Chai Y, Schrooten J, et al. The combined mechanism of bone morphogenetic protein-and calcium phosphate-induced skeletal tissue formation by human periosteum derived cells. *Eur Cell Mater*. 2016b;30:11–25.
31. Chai YC, Roberts SJ, Schrooten J, Luyten FP. Probing the osteoinductive effect of calcium phosphate by using an in vitro biomimetic model. *Tissue Eng Part A*. 2010;17(7–8):1083–97.
32. Ducheyne P, Radin S, King L. The effect of calcium phosphate ceramic composition and structure on in vitro behavior. I. Dissolution. *J Biomed Mater Res*. 1993;27(1):25–34.
33. Vallet-Regí M, González-Calbet JM. Calcium phosphates as substitution of bone tissues. *Prog Solid State Chem*. 2004;32(1):1–31.
34. Ghavimi SAA, Ebrahimzadeh MH, Shokrgozar MA, Solati-Hashjin M, Osman NAA. Effect of starch content on the biodegradation of polycaprolactone/starch composite for fabricating in situ pore-forming scaffolds. *Polym Test*. 2015;43:94–102.
35. Lee JB, Lee SH, Yu SM, Park J-C, Choi JB, Kim JK. PLGA scaffold incorporated with hydroxyapatite for cartilage regeneration. *Surf Coat Technol*. 2008;202(22):5757–61.
36. Rezwani K, Chen Q, Blaker J, Boccaccini AR. Biodegradable and bioactive porous polymer/inorganic composite scaffolds for bone tissue engineering. *Biomaterials*. 2006;27(18):3413–31.
37. Edlund U, Albertsson A-C. Polyesters based on diacid monomers. *Adv Drug Deliv Rev*. 2003;55(4):585–609.
38. Ulery BD, Nair LS, Laurencin CT. Biomedical applications of biodegradable polymers. *J Polym Sci B Polym Phys*. 2011;49(12):832–64.
39. Yang F, Wolke J, Jansen J. Biomimetic calcium phosphate coating on electrospun poly (ϵ -caprolactone) scaffolds for bone tissue engineering. *Chem Eng J*. 2008;137(1):154–61.
40. Moreau JL, Xu HH. Mesenchymal stem cell proliferation and differentiation on an injectable calcium phosphate-chitosan composite scaffold. *Biomaterials*. 2009;30(14):2675–82.
41. Wheelton A, Mace J, Khan WS, Anand S. Biomaterials and fabrication to optimise scaffold properties for musculoskeletal tissue engineering. *Curr Stem Cell Res Ther*. 2016;11(7):578–84.
42. Tadic D, Epple M. A thorough physicochemical characterisation of 14 calcium phosphate-based bone substitution materials in comparison to natural bone. *Biomaterials*. 2004;25(6):987–94.
43. Samavedi S, Whittington AR, Goldstein AS. Calcium phosphate ceramics in bone tissue engineering: a review of properties and their influence on cell behavior. *Acta Biomater*. 2013;9(9):8037–45.
44. Fulda S, Gorman AM, Hori O, Samali A. Cellular stress responses: cell survival and cell death. *International journal of cell biology*. 2010;2010.
45. Zhan F, Watanabe Y, Shimoda A, Hamada E, Kobayashi Y, Maekawa M. Evaluation of serum bone alkaline phosphatase activity in patients with liver disease: comparison between electrophoresis and chemiluminescent enzyme immunoassay. *Clinica Chimica Acta*. 2016.